USING NEW TECHNOLOGY TO ENHANCE THE WARNING PROCESS FOR A DEADLY WET MICROBURST IN EASTERN COLORADO

Ronald T. Holmes

National Weather Service Forecast Office
Sioux Falls, South Dakota

David A. Imy

National Weather Service Forecast Office
Denver, Colorado

Abstract

On 16 July 1993, thunderstorms developed across northeast Colorado during the late afternoon hours. Most of the storms were short-lived and non-severe. However, one storm persisted for about 3 hours and briefly evolved into a supercell. This storm produced golf ball-sized hail and winds estimated up to 130 knots. The ferocious downburst winds annihilated a mobile home and killed one of its three occupants. Emphasis is placed on how the use of advanced mesoscale models and WSR-88D data diagnosed mesoscale features which contributed to the intensification of this isolated thunderstorm. Real time use of these new technologies to enhance the warning process is explored.

1. Introduction

On 16 July 1993, an isolated wet microburst produced strong winds and large hail in northeast Colorado. Severe winds accompanying the storm destroyed an anchored mobile home, resulting in one fatality and two injuries. An investigation by National Weather Service (NWS) personnel estimated wind speeds up to 130 kt (66.9 m s^{-1}) based on the resultant damage (USDC 1993).

Analyses from two mesoscale models are used to pinpoint where the best conditions for severe convection were present. Also included are significant storm features as observed by the Weather Surveillance Radar—1988 Doppler (WSR-88D) system (Crum and Alberty 1993). We show how this new technology helped forecasters anticipate severe weather in a local area. Once this threat was recognized, forecasters were able to provide statements and accurate warnings to highlight the developing severe weather for the public.

2. Model Descriptions

Two mesoscale models were used to analyze this event. These models, developed at NOAA Forecast Systems Laboratory (FSL), have proven to be useful to the Denver (DEN) NWS forecasters because they generate analyses and forecasts on a finer spatial and temporal scale than current conventional models.

a. MAPS

The first model is the Mesoscale Analysis and Prediction System (MAPS; Benjamin et al. 1991). MAPS provides mesoscale analyses of surface and upper-air parameters across the continental United States. It incorporates hourly surface observations, wind profiler data, aircraft reports typically made every

7.5 minutes, and data from rawinsondes for its analyses and forecasts. The three-dimensional grid contains 24 layers in the vertical (5 terrain-following sigma layers and 19 isentropic layers), with a horizontal resolution of 60 km.

Hourly output from MAPS consists of conventional surface analyses and derived products (Table 1). Every three hours an analysis of mandatory pressure levels and 3- and 6-hour forecasts are produced. At 0000 UTC and 1200 UTC, 3-, 6-, 9-, and 12-hour forecasts are also generated. Analyses and forecasts are available on both isobaric and isentropic surfaces, and can be displayed in cross section format. Further details concerning the MAPS model can be found in Bleck and Benjamin (1993).

b. LAPS

The second model is the Local Analysis and Prediction System (LAPS; McGinley et al. 1991). LAPS has a 10 km horizontal and 50 mb vertical resolution. Input to LAPS includes standard surface observations, mesonet data, wind profiler observations, and aircraft data. Satellite information is used in the surface temperature analysis and the three dimensional moisture and cloud analyses. Doppler radial velocities are used to generate wind vectors. This model also outputs gridded fields of conventional surface and upper-level analyses as well as a variety of derived products at one-hour intervals (Table 2). Forecasts of these fields are currently not available.

3. Synoptic Environment

The synoptic environment for large scale lift over Colorado at 0000 UTC 17 July was weak. The dominant feature was a large anticyclone in the mid-troposphere that covered most of the central United States (Fig. 1). On the west side of this ridge, a very weak short wave trough was moving across Colorado. Relatively light winds at the mid-levels resulted in neutral to weak cold advection behind the short wave and there was only weak warm advection in the low levels. In the upper troposphere (not shown), a moderately strong jet streak prevailed over Wyoming and Montana, but the divergence associated with this jet was located too far north to affect Colorado. At the surface a weak cold front was moving south across Wyoming and Nebraska during the day.

Doswell (1985, 1987) pointed out that synoptic scale features do not trigger deep moist convection but are responsible for maintaining a favorable thermodynamic profile in which convection may form. This can be achieved through synoptic scale lift or favorable differential temperature advection. The synoptic environment on this day featured only weak lift and differential temperature advection which was enough to keep lapse

Table 1. Output from MAPS model available at NWSFO Denver

CONSTANT PRESSURE	ISENTROPIC SURFACE	LAYER	SURFACE
HEIGHT	MONTGOMERY STREAM FUNCTION	THICKNESS	MSL PRESSURE
HEIGHT CHANGE	ADIABATIC OMEGA	VERTICAL TEMPERATURE CHANGE	3-HR PRESSURE CHANGE
VORTICITY	VORTICITY	Q-VECTORS	WINDS
VORTICITY ADVECTION	VORTICITY ADVECTION	Q-VECTOR DIVERGENCE	TEMPERATURE
DIVERGENCE	DIVERGENCE	Q_N-DIVERGENCE	DEWPOINT
DEFORMATION VECTORS	DEFORMATION VECTORS	Q_S-DIVERGENCE	DEWPOINT DEPRESSION
TOTAL DEFORMATION	TOTAL DEFORMATION	PRECIPITABLE WATER	LIFTED INDEX
WINDS	WINDS	CONVECTIVE AVAILABLE POTENTIAL ENERGY	MOISTURE CONVERGENCE
STREAMLINES	STREAMLINES	CONVECTIVE INHIBITION	POTENTIAL TEMPERATURE
ISOTACHS	ISOTACHS		EQUIVALENT POTENTIAL TEMPERATURE
GEOSTROPHIC WINDS	GEOSTROPHIC WINDS		TEMPERATURE ADVECTION
AGEOSTROPHIC WINDS	AGEOSTROPHIC WINDS		RELATIVE VORTICITY
TEMPERATURE	TEMPERATURE		
TEMPERATURE ADVECTION	POTENTIAL VORTICITY		
POTENTIAL TEMPERATURE	POTENTIAL VORTICITY ADVECTION		
EQUIVALENT POTENTIAL TEMPERATURE	PRESSURE		
LAPSE RATE	LAPSE RATE		
Q-VECTORS	RELATIVE HUMIDITY		
Q-VECTOR DIVERGENCE	DEWPOINT		
GEOSTROPHIC FRONTOGENESIS	SPECIFIC HUMIDITY		
RELATIVE HUMIDITY	MOISTURE ADVECTION		
DEWPOINT	MOISTURE CONVERGENCE		
SPECIFIC HUMIDITY	CONDENSATION PRESSURE		
MOISTURE ADVECTION	CONDENSATION PRESSURE DEFICIT		
MOISTURE CONVERGENCE			
CONDENSATION PRESSURE			
CONDENSATION PRESSURE DEFICIT			
ICING			

rates conditionally unstable. The MAPS 700-500 mb lapse rate analysis for 1800 UTC (not shown) indicated lapse rates of 8 to 9 °C km^{-1} over the region.

4. Mesoscale Environment

Toth and Johnson (1984) have described a distinct climatological summertime wind flow near the eastern foothills of the Colorado Rocky Mountains linked to the mountain-valley circulation. This diurnal wind flow is comprised of low-level easterly upslope flow which develops in the early morning and increases in depth during the afternoon. Both Modahl (1979) and Doswell (1980) have shown that increasing upslope flow

plays an important role in the production of severe weather over the high plains because it decreases low-level stability. The Platteville wind profiler (Fig. 2), located about 50 km north of DEN, revealed low-level easterly flow developing between 1600 and 1800 UTC 16 July which increased in depth by 2200 (unfortunately data from 1900 to 2100 UTC was missing). The easterly flow also aided the transport of relatively higher moisture values from the Central Plains into northeast Colorado. This resulted in a narrow equivalent potential temperature (θ_e) ridge oriented east to west (Fig. 3) with a large θ_e gradient across northeast Colorado.

The Denver rawinsonde observation (Fig. 4) for 0000 UTC 17 July shows a deep layer of dry air in the low layers with

Table 2. LAPS model output available at NWSFO Denver

ANALYZED	DERIVED
3-HR PRESSURE CHANGE	LIFTED INDEX
1500 METER PRESSURE	DIVERGENCE
WIND BARBS	MOISTURE CONVERGENCE
WIND SPEED	MOISTURE ADVECTION
TEMPERATURE	TEMPERATURE ADVECTION
DEWPOINT	POTENTIAL TEMPERATURE ADVECTION
RELATIVE HUMIDITY	VORTICITY
MIXING RATIO	VERTICAL VELOCITY
POTENTIAL TEMPERATURE	COLORADO SEVERE STORMS INDEX
EQUIVALENT POTENTIAL TEMPERATURE	CONVECTIVE AVAILABLE POTENTIAL ENERGY
SURFACE VISIBILITY	CONVECTIVE INHIBITION

moisture in the mid-levels. This moisture stratification has been shown by Wakimoto and Bringi (1985) to be conducive to dry microburst type thunderstorms. The convective available potential energy (CAPE) was low (9 J kg^{-1}) and the convective inhibition (CIN) was high (-30 J kg^{-1}) as a result of the dry low-level air and a cap around 400 mb. The CIN represents the energy needed for a parcel to overcome any negative area below the LFC in order to tap the available potential energy (Colby 1984). This combination of low CAPE and high CIN indicated that the atmosphere was too stable for thunderstorm development near Denver.

The LAPS model, with its better spatial resolution over conventional surface data, showed that the low-level moisture distribution over northeast Colorado was quite different. Figure 5 shows the LAPS surface analysis of wind and dew point for 0000 UTC 17 July. There was a large moisture gradient, with unusually high dew points for Colorado, located east of a Fort Collins (FCL) to Denver (DEN) to Limon (LIC) line where readings were in the low 60's (F).

During the afternoon, low-level moisture increased just to the north and west of Akron, Colorado (AKO) due to prolonged moisture flux convergence. Figures 6a and 6b show the LAPS analysis of surface moisture flux convergence for 1800 UTC 16 July and 0000 UTC 17 July, respectively. East to southeast
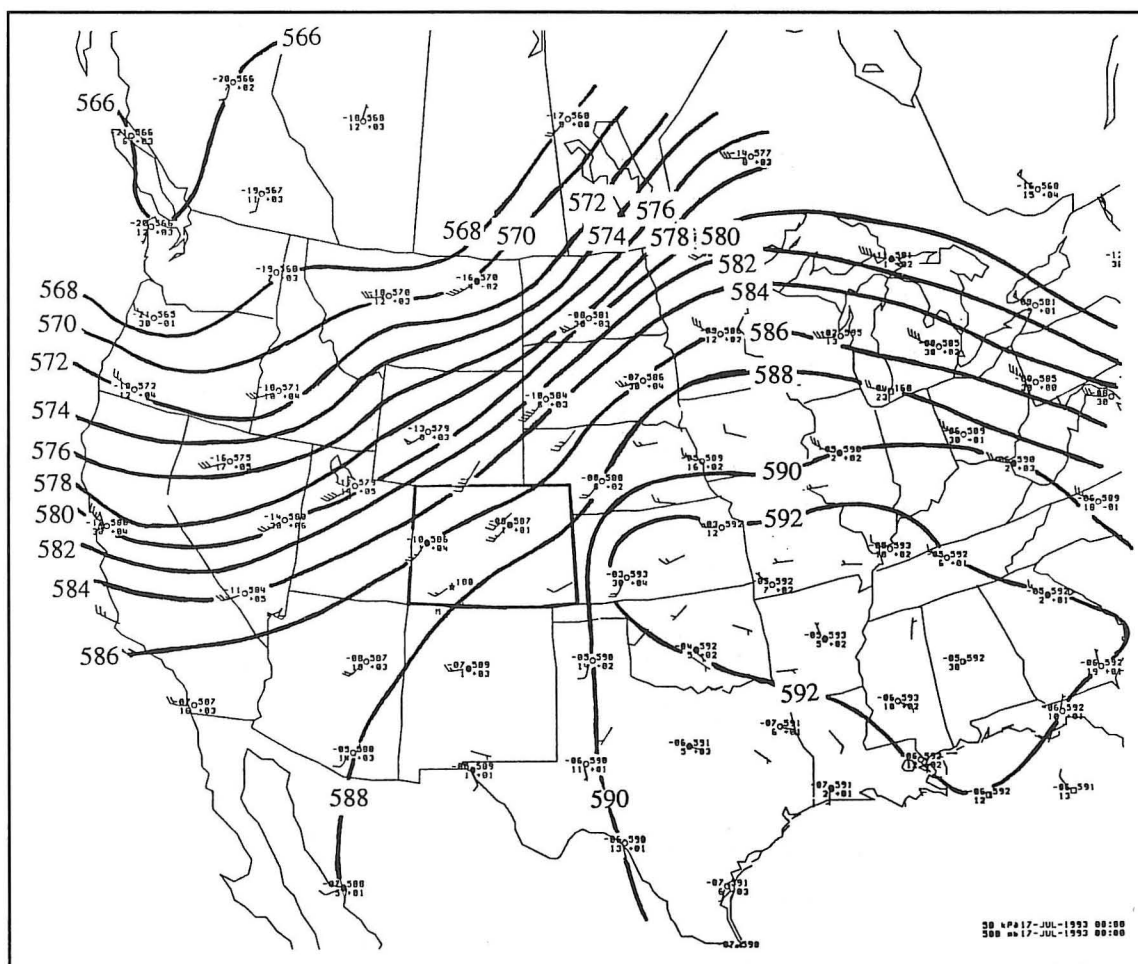

Fig. 1. 0000 UTC 17 July 1993 500-mb height analysis (contours every 20 m) along with rawindsonde and profiler plots (kt).
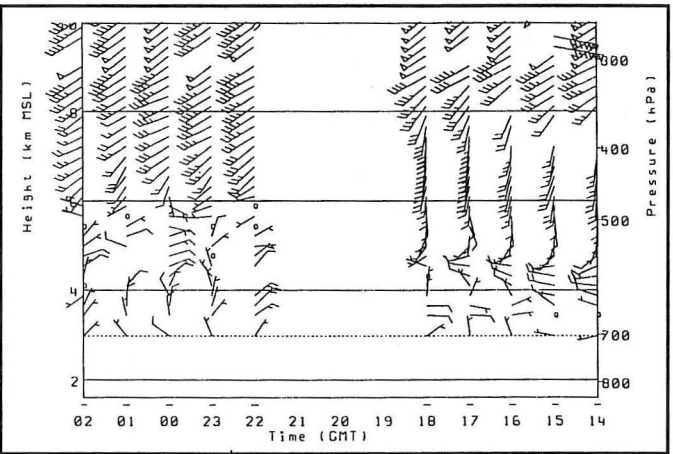
Fig. 2. Platteville (CO) wind profiler time series from 1400 UTC 16 July to 0200 UTC 17 July 1993. Wind speed in knots. Time increases from right to left.
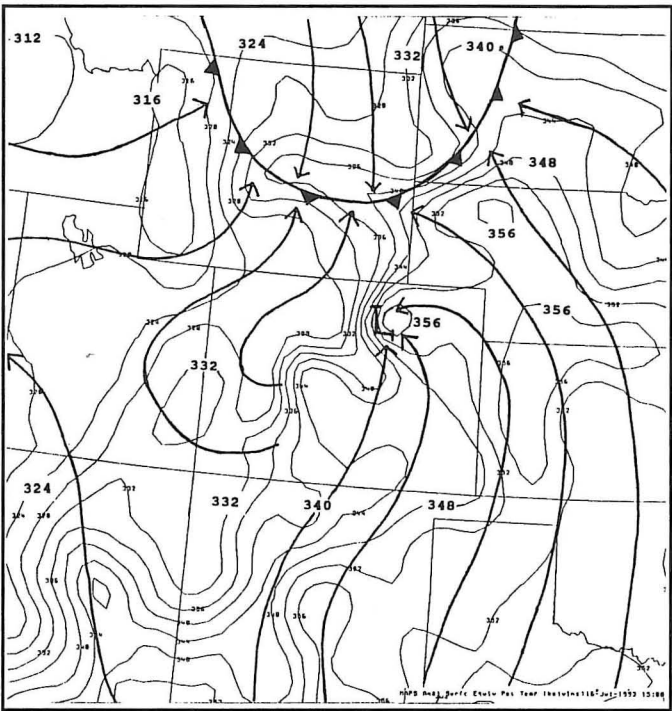

Fig. 3. MAPS analysis of surface equivalent potential temperature (°K) and streamlines (arrows) for 1500 UTC 16 July 1993. "L" denotes position of surface circulation over northeast Colorado.
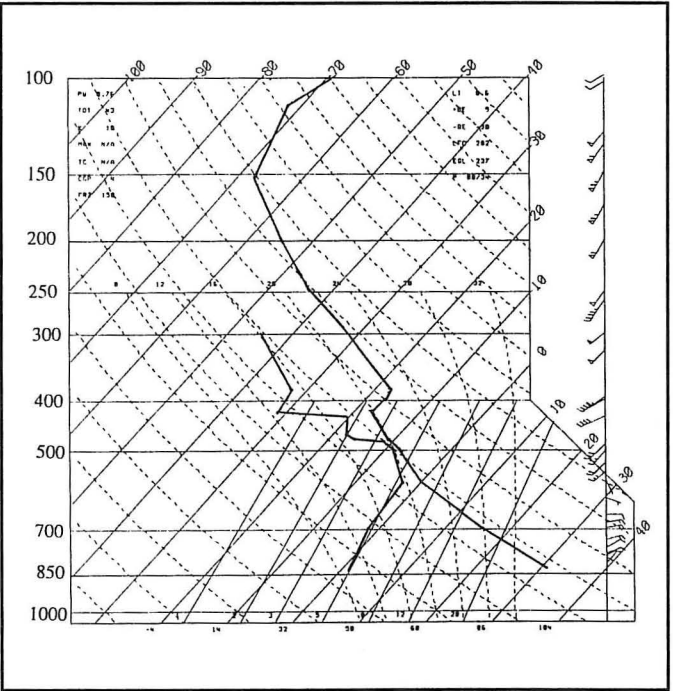

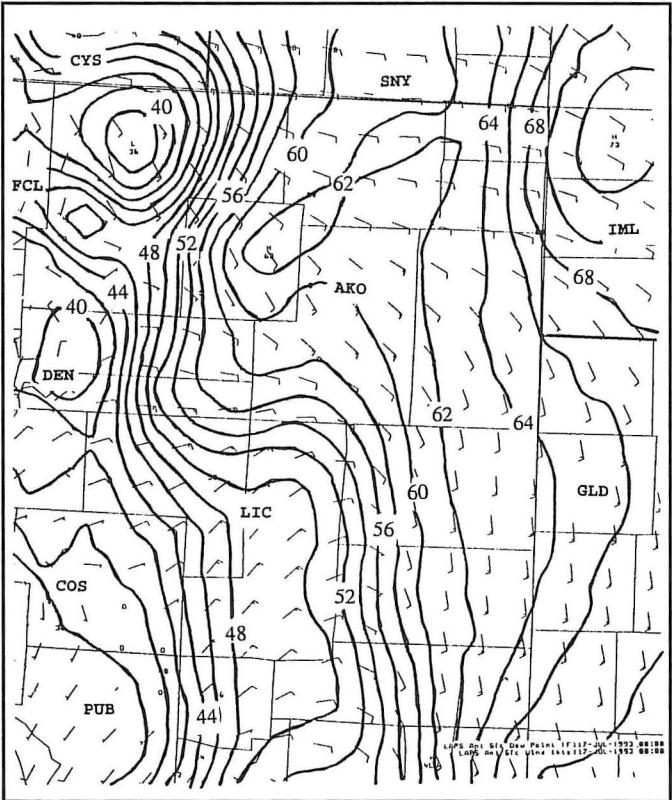Fig. 4. Denver sounding for 0000 UTC 17 July 1993.
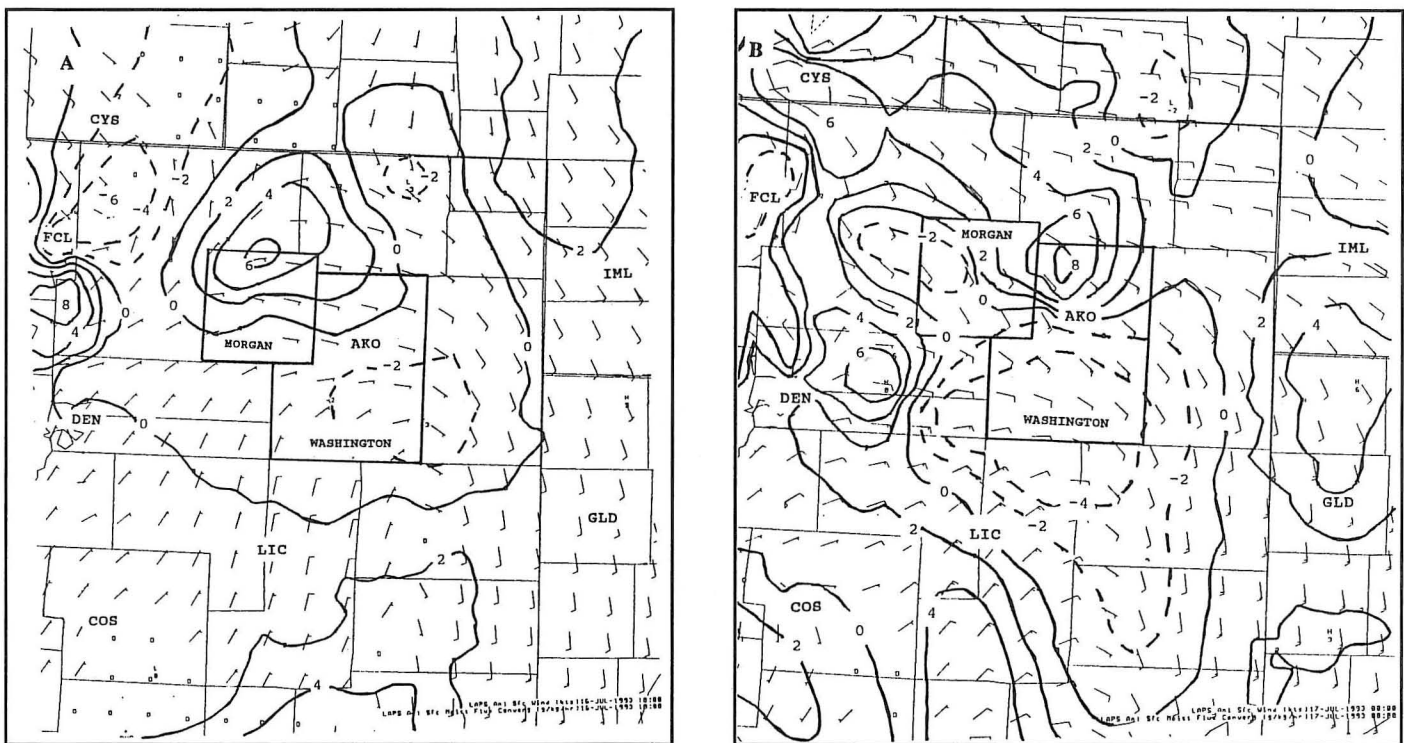

Fig. 5. LAPS surface dew point (F) and surface wind (kt) for 0000 UTC 17 July 1993.

Fig. 6. LAPS surface moisture flux convergence (g kg^{-1} hr^{-1}) and surface wind (kt) for (a) 1800 UTC 16 July 1993 and (b) 0000 UTC 17 July 1993.

surface winds were aiding the transport of low-level moisture from the Central Plains into northeast Colorado. A maximum of surface moisture flux convergence was located over northern Morgan county at 1800 UTC. This maximum persisted for another 6 hours and was located over northwest Washington county (where the thunderstorm eventually intensified into a supercell) at 0000 UTC. This persistent moisture flux convergence likely caused low-level moisture to deepen with time in this local area.

To investigate this deepening moisture, a vertical cross section of mixing ratio was generated using the LAPS model. The cross section was oriented west to east across northern Colorado (Fig. 7a). Figures 7b and 7c show the cross section analyses of winds and mixing ratio for 2100 UTC 16 July and 0000 UTC 17 July, respectively. Surface mixing ratio values near the developing storm (position of arrow at 2100 and 0000 UTC) increased from 6 to 12 g kg^{-1} between 2100 UTC 16 July and 0000 UTC 17 July. This increase was due to a combination of the storm moving east into better moisture and moisture deepening with time due to persistent moisture flux convergence.

The unusually high moisture values at low-levels resulted in a maximum of CAPE (Fig. 8) and a minimum of CIN (Fig. 9) over Morgan and Washington counties[1]. Forecasters at DEN have been using the LAPS CIN chart operationally since 1991.

----

[1]The discrepancy between CAPE and CIN on the 0000 UTC DEN sounding and the LAPS analysis of CAPE and CIN over Denver is the result of different methods used to calculate these parameters and the different vertical resolution between the Denver sounding and the LAPS model.

They have noticed that as values approach 0 to -5 J kg^{-1} the likelihood for convection increases given other favorable conditions for convection. The CIN values indicated that a cap would suppress widespread convection over much of northeast Colorado except for a small area in Washington county where the thunderstorm became severe.

5. Significant Radar Features, Severe Weather and Warnings

Scattered convection developed across Wyoming and Nebraska as a cold front advanced south during the afternoon of 16 July 1993. A few thunderstorms developed northeast of Denver during the afternoon hours but the storms were weak and short lived. One storm developed about 90 km northeast of DEN shortly before 2100 UTC along a weak outflow boundary generated by previous convection. The maximum reflectivity associated with this storm reached 50 dBZ by 2133 UTC (Fig. 10) but the storm did not exhibit any severe weather signatures (Lemon 1980).

As this storm moved slowly east during the next hour the boundary on which it developed was pushed south and west due to the storm's outflow (Fig. 11). Meanwhile, an outflow boundary that had originated with a strong thunderstorm in southwest Nebraska was moving south toward this non-severe thunderstorm. One of the advantages of the WSR-88D radar over conventional radars is its ability to detect fine boundaries at distant ranges. Assuming a standard refractive index, the DEN WSR-88D indicated that this second boundary had a depth to 3 km. This boundary was located north of the thunderstorm at 2219 UTC, but by 2254 UTC, the boundary was approaching
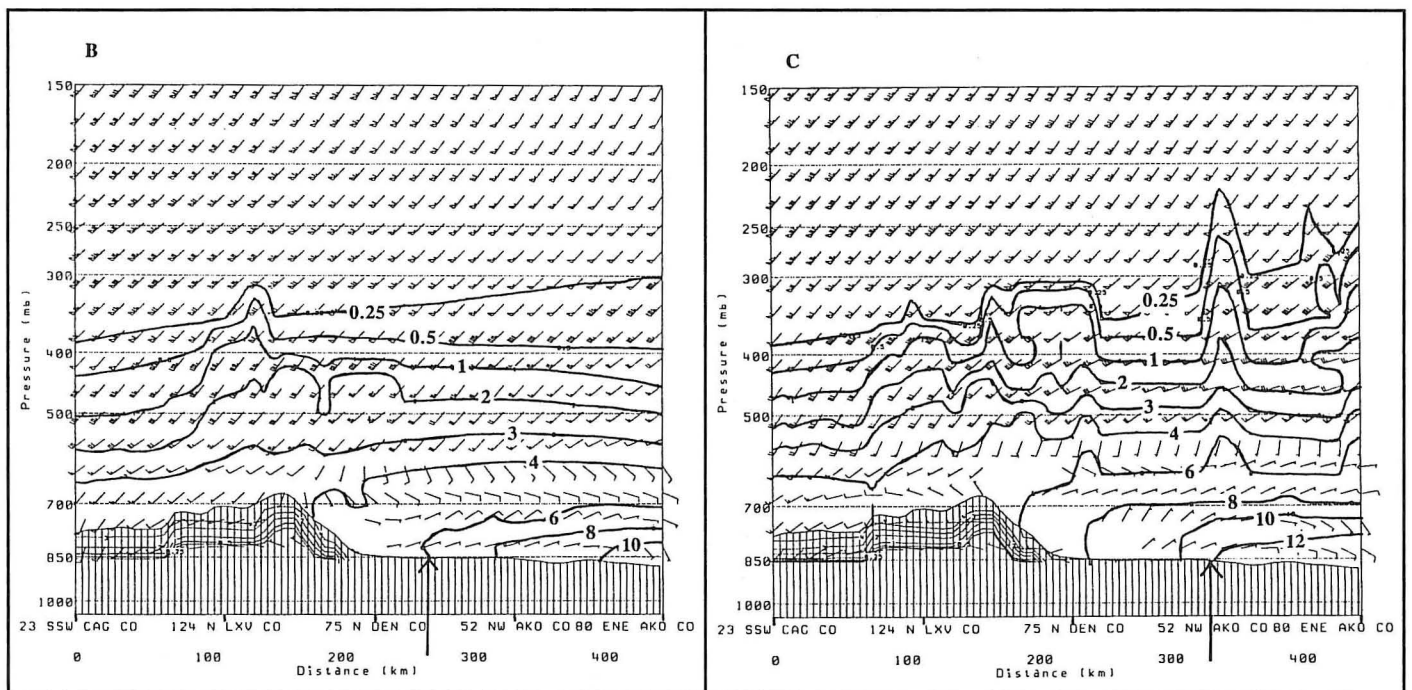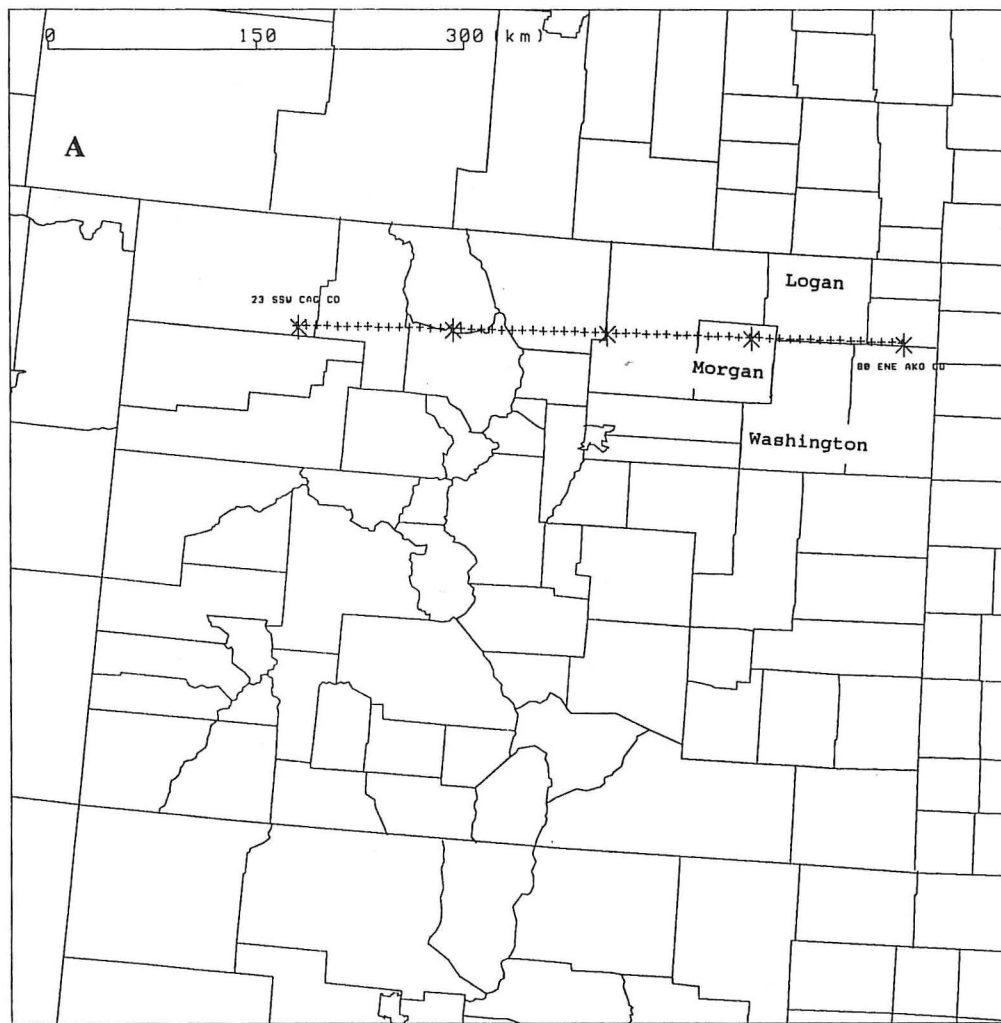
Fig. 7. LAPS cross section of winds (kt) and mixing ratio (g kg⁻¹): (a) orientation of cross section from west to east across northern Colorado, (b) 2100 UTC 16 July 1993 and (c) 0000 UTC 17 July 1993. Arrows indicate approximate location of storm for the time listed.
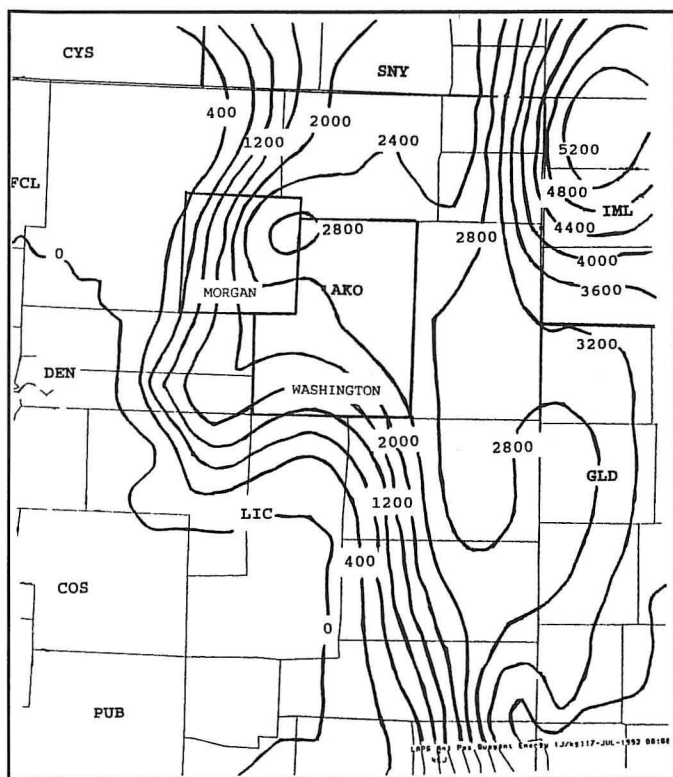
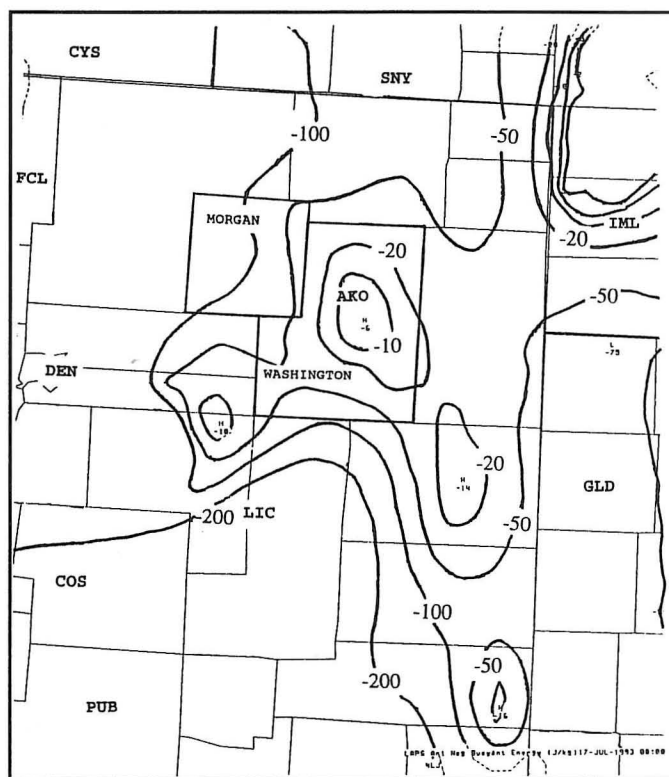Fig. 8. LAPS convective available potential energy (CAPE J kg⁻¹) for 0000 UTC 17 July 1993.

Fig. 9. LAPS convective inhibition (CIN J kg⁻¹) for 0000 UTC 17 July 1993.
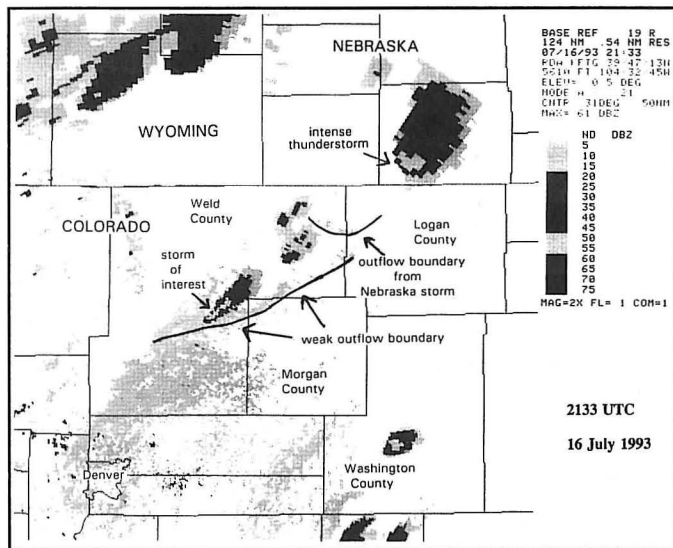

Fig. 10. DEN WSR-88D 0.5° elevation angle .54 nm resolution base reflectivity (dBZ) for 2133 UTC 16 July 1993. Outflow boundary from strong thunderstorm in Nebraska is detected moving southward through northeast Weld and northwest Logan counties.
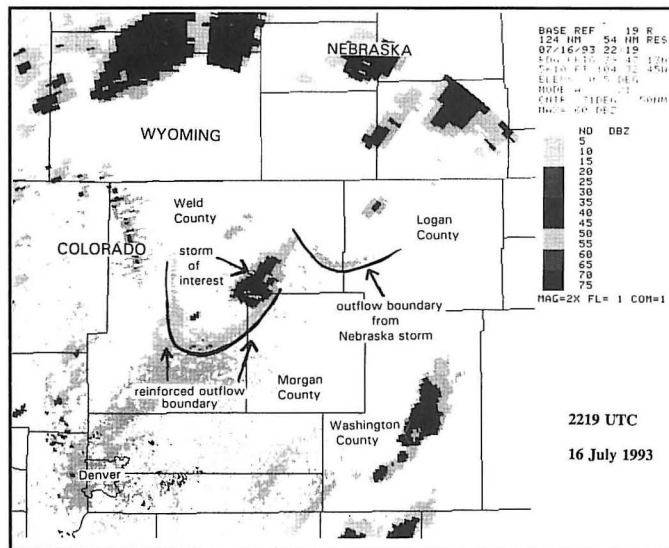

Fig. 11. As in Fig. 10 except for 2219 UTC. Outflow from Nebraska thunderstorm continues to move southward.
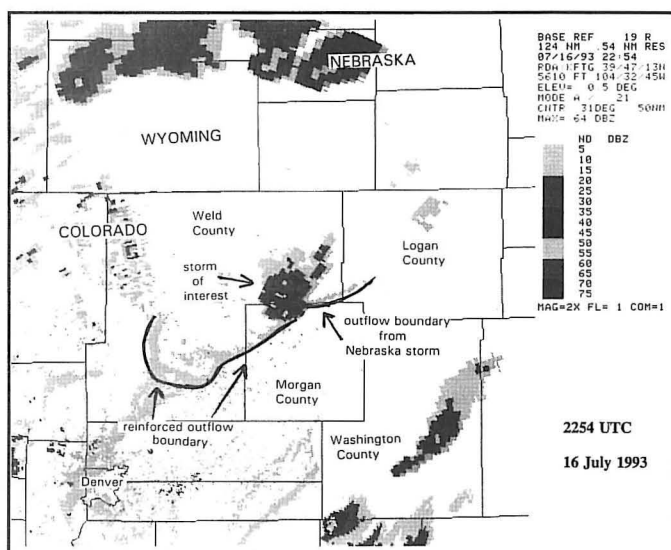
Fig. 12. As in Fig. 10 except for 2254 UTC. Nebraska outflow boundary close to intersecting the updraft portion of the non-severe thunderstorm in northwest Morgan County.
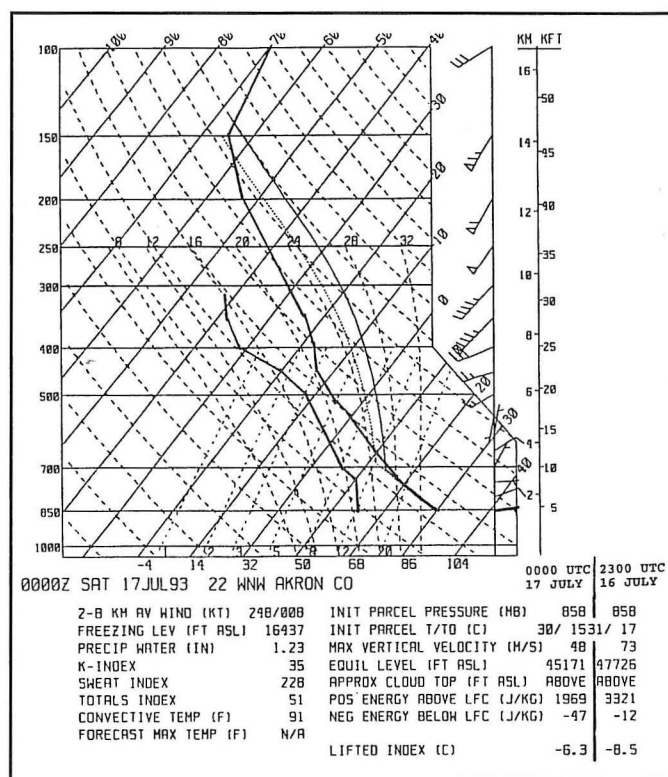

Fig. 13. LAPS sounding 22 km west northwest of AKO (125 km northeast of Denver) for 0000 UTC 17 July 1993. Table below lists calculated parameters based on a lifted parcel using the 0000 UTC 17 July AKO surface temperature and dew point. Last column lists modified parameters using the 2300 UTC 16 July AKO surface temperature and dew point.

the southern portion of the storm near the updraft region (Fig. 12). The second boundary became more difficult to see on radar since it was becoming more shallow with time, but it appears that the boundary intersected the updraft region of the storm around 2300 UTC (not shown). After this intersection, the storm began to intensify.

To gain a further understanding of the vertical moisture and temperature profile that this intensifying thunderstorm was ingesting, forecasters generated a sounding near the storm's location using the LAPS model. Since LAPS inputs the most recent Doppler radar data, aircraft reports, wind profiler data, and satellite data, it is a more powerful tool than the Sounding and Hodograph Application Research Program (SHARP) (Hart and Korotky 1991) because it generates a sounding, using the latest gridded data, for any location independent of a RAOB site. Figure 13 is the 0000 UTC 17 July 1993, LAPS model sounding for this location (22 km west northwest of AKO or 125 km northeast of Denver) where the storm intensified (hereafter referred to as the AKO ''sounding''). The table of information at the bottom represents computed parameters based on the initial LAPS surface temperature and dew point (taken from the 0000 UTC AKO surface observation) of 87 °F and 59 °F, respectively. The atmosphere was moderately unstable with a CAPE of 1969 J kg^{-1}, but the CIN was high enough (-47 J kg^{-1}) to prevent convection from forming without an additional lifting mechanism. Modifying the sounding using the observed 2300 UTC AKO surface temperature and dew point of 87 °F and 63 °F degrees, respectively, accounts for the highest temperature and dew point observed at AKO as the supercell was intensifying. Using these values, the CAPE increased to 3321 J kg^{-1}, indicative of strong instability. The CIN also decreased (-12 J kg^{-1}), indicating that only weak mesoscale lift was needed in this local environment to break the cap.

The AKO sounding differed from the DEN sounding in that it showed a wet microburst environment. There was a deep layer of moisture in the lower troposphere comprised of high equivalent potential temperature (θ_e). In the mid and upper

levels drier air was in place resulting in a steep lapse rate of θ_e ($\Delta\theta_e = 28$ °K). Atkins and Wakimoto (1991) showed that on wet microburst days the difference in θ_e between the surface and mid levels was ≥ 20 °K. This represented a convectively unstable environment favorable for generating strong microbursts. Dry air at mid levels is effective in generating large values of negative buoyancy due to melting hail and evaporational cooling (Srivastava 1985; Wakimoto and Bringi 1988; Atkins and Wakimoto 1991). The negative buoyancy is enhanced in a wet microburst environment by water loading.

To investigate the strength of the estimated winds, a calculation of the downdraft potential within this wet microburst environment was performed using the method of Foster (1958) and Caracena and Maier (1987). The 400 to 600 mb layer was chosen as the downdraft genesis region because it contained the lowest θ_e air which represented the greatest evaporational cooling potential. It was also assumed that the downdraft air remained saturated as it descended toward the surface and that it translated directly into a horizontal wind upon hitting the ground. The buoyancy equation was integrated from the level of free sink to the surface to estimate peak wind gusts. The result was a calculated downdraft speed of 95 kt. Added to this was a storm motion of 10 kt which yielded a total horizontal wind of 105 kt. This is reasonably close to the 130 kt winds estimated from the storm damage survey.

From the LAPS data it was clear that the thermodynamic properties over northeast Colorado were very much different from those along the Rocky Mountain foothills. Forecasters

looking at the DEN sounding analysis alone might have been fooled into thinking the threat for severe thunderstorms over northeast Colorado was negligible due to the low CAPE and strong cap. However, LAPS showed forecasters that strong thunderstorms with gusty winds and heavy rain were likely in a localized area near northern Morgan and Washington counties. The severe weather forecaster recognized this potential and issued a special weather statement an hour prior to the microburst to highlight the threat of near-severe thunderstorms in this area. The statement mentioned the possibility of heavy rain, gusty winds, and hail. However, at the time, neither the DEN WSR-88D system nor the WSR-57 radar at Limon, Colorado (LIC) indicated that this storm was severe. Also, several spotters located close to the storm did not see any visual signs of severe weather.

Browning (1965) showed that severe weather is more likely when thunderstorms possess weak echo regions (WER), or bounded weak echo regions (BWER's), and high reflectivities aloft. Lemon (1980) developed a technique to volumetrically investigate for the existence of WER's and BWER's. Several cases (e.g., Imy and Pence 1992; Przybylinski et al. 1992) have illustrated the effectiveness of using tilt methods to identify WER's and BWER's in severe and tornadic storms. The forecasters were examining four slices of reflectivity and velocity from the KFTG WSR-88D radar as this storm continued to intensify. At 2346 UTC (Fig. 14), the reflectivities aloft increased rapidly with $60+$ dBZ extending vertically to 10 km. The mid-level echo overhang became more expansive and extended 5 km beyond a strong low-level reflectivity gradient on the southeast side of the storm indicating a WER.

A mid-level circulation was observed in the four separate elevations of velocity data and, using Donaldson's (1970) criteria, a mesocyclone existed in the mid-levels of the storm from approximately 2345 UTC until 0015 UTC. The highest rotational velocities, however, were around 15 m s^{-1}, which, by Burgess and Lemon's (1990) criteria, would rate this mesocyclone as weak. Given the weak mesocyclone and a storm-relative helicity less than 100 m^2 s^{-2} near the storm's location

(based on the AKO sounding), the forecasters determined that tornadoes were not likely at this time. Burgess and Lemon (1990) found that over 90% of all mesocyclonic storms produce some type of severe weather (i.e., hail, wind, and/or tornado), but only about one-third spawned tornadoes. With this in mind the forecasters determined that large hail would be the main threat due to high theta-e values, the WER, high reflectivities aloft, and high VIL values. The presence of dry air in the mid levels over deep low-level moisture on the AKO sounding also suggested the potential for damaging winds from a "wet" microburst. Thus, the severe weather forecaster issued a severe thunderstorm warning at 2345 UTC valid until 0015 UTC for northeast Morgan county. At 0010 UTC the first severe weather report with this storm came from a spotter who measured golf ball sized hail in northeast Morgan county.

As the severe thunderstorm moved slowly east and intensified, a reflectivity notch developed on the southeast side of the storm at 0009 UTC (Fig. 15—note that all reflectivities below 24 dBZ have been removed). This low-level concavity at 0.5° is bounded on three sides by reflectivities of $50+$ dBZ giving the storm a hook appearance. Higher reflectivities are noted above the low-level concavity with 50 dBZ at 2.4° and $60+$ dBZ at 3.4°. A reflectivity maximum of 73 dBZ was located at 3.4° just northwest of the low-level concavity. The mid-level circulation was still present but was broad with no signs of tightening or strengthening so the forecasters elected to issue another severe thunderstorm warning instead of a tornado warning. Input to this decision also came from storm spotters near the storm who did not observe rotation or indications of tornadic development. This new warning was for southwest Logan, northeast Morgan, and northwest Washington counties from 0015 to 0100 UTC.

Since this storm did possess a weak mesocyclone, strong reflectivity at great heights, and very high VIL values (96 kg m^{-2} at 0015 UTC), the following sentence was added to the warning: "This storm is capable of producing wind damage, golf ball or larger hail, and brief heavy rain. Take Cover now!"
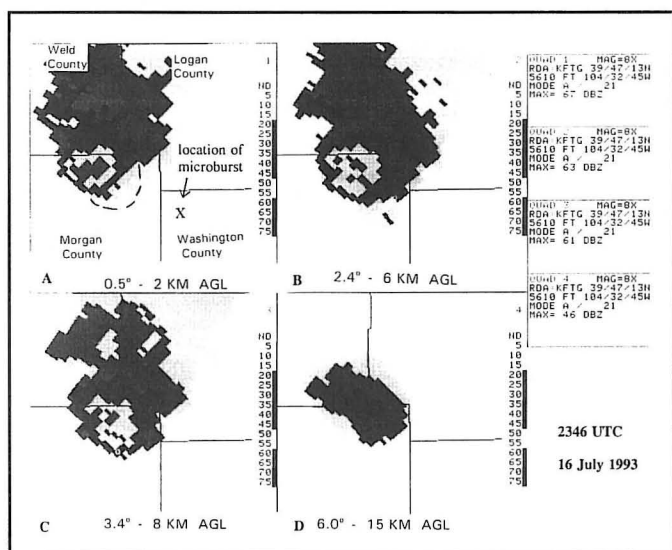

Fig. 14. DEN WSR-88D .54 nm resolution base reflectivity (dBZ) at 2346 UTC 16 July 1993 for (a) 0.5°, (b) 2.4°, (c) 3.4° and (d) 6.0° elevation angle showing a WER. Dashed line in (a) indicates extent of reflectivity overhang (dBZ>35) from 3.4° elevation.
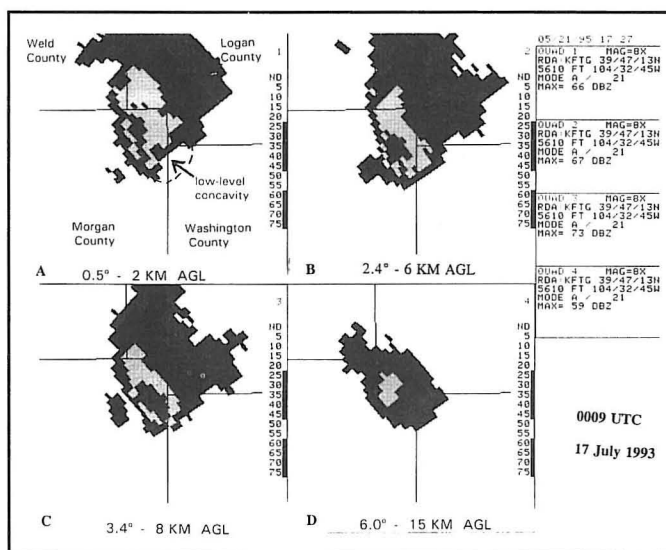

Fig. 15. As in Fig. 14 except for 0009 UTC 17 July 1993. A low-level concavity has developed at 0.5° bounded above by $70+$ dBZ at 3.4° indicating a WER.

At 0030 UTC, 1.75 inch (4.4 cm) diameter hail was reported near the microburst location.

Another product from the WSR-88D that helped determine the severity of this storm was the Vertically Integrated Liquid (VIL) product (Green and Clark 1972; Klazura and Imy 1993). The VIL values represent reflectivity data that have been converted to liquid water equivalent values through an empirically derived relationship. VIL's have been found to be a reliable indicator of severe hail when environmental conditions are taken into account (Winston and Ruthi 1986). Little documentation exists, however, for using the VIL product to determine the microburst potential.

In this case, as the storm intensified, the maximum VIL values increased from 30 kg m^{-2} to 60 kg m^{-2} from 2311 UTC to 2334 UTC (Fig. 16). The VIL values continued to increase and were >75 kg m^{-2} from 2352 UTC to 0021 UTC. The VIL maximum for this storm was 96 kg m^{-2} at 0015 UTC with 60+ dBZ reflectivities extending vertically to 16 km. The VIL maximum decreased rapidly after 0015 UTC dropping to 65 kg m^{-2} by 0027 UTC. This period also marked the collapse of the WER (Figs. 17 and 18). Simultaneously, the vertical height of the 60+ dBZ maximum reflectivity core dropped to 10 km and the low-level reflectivity increased in intensity as reflectivity at 3.4° diminished. The low-level concavity disappeared with the mid-level overhang becoming non-existent.

The time of the microburst was estimated around 0030 UTC. Figures 19 and 20 show the number of 4 km × 4 km VIL boxes with values greater than 45 kg m^{-2} and 60 kg m^{-2}, respectively. The areal coverage of these higher VIL values decreased by more than 50 percent along with rapidly decreasing VIL values from 0015 UTC to 0027 UTC. The decrease in VIL signaled the descent of the high reflectivity core that had been held aloft earlier by the strong WER. This case suggests that a dramatic increase in VIL followed by a rapid decrease in VIL values might be another precursor forecasters can use, in conjunction with traditional methods of determining severe storms (Lemon 1980), to signal the potential for severe microburst winds. As our experience with the WSR-88D technology grows forecasters should continue to test this idea.

During the microburst, winds estimated up to 130 kt and golf ball sized hail fell in extreme northwest Washington County in a very sparsely populated area. Unfortunately, the fury of this storm was unleashed on an anchored mobile home which was picked up and tossed 15 m before being slammed to the ground and destroyed. A man was killed and his pregnant wife and child were injured. A post storm survey noted that a 4 mile long by 2 mile wide swath of damage, mostly flattened corn crops, clearly marked the track of this deadly microburst. Storm damage survey revealed that the strongest winds were perpendicular to the radials of the DEN WSR-88D radar. Since the WSR-88D radar cannot detect winds that blow perpendicular to the radial there was no way of determining the severity of these winds in real time.

6. Conclusion

The deadly severe thunderstorm of 16 July 1993 was analyzed using a combination of conventional data sources and new technology. By using mesoscale models such as MAPS and LAPS, with their enhanced spatial and temporal resolution, forecasters were able to more closely monitor changing conditions in the mesoscale environment over northeast Colorado than conventional data would have revealed.

The standard rawinsonde observation at DEN showed the atmosphere along the Rocky Mountain foothills was unrepresentative of the environment in which this severe thunderstorm
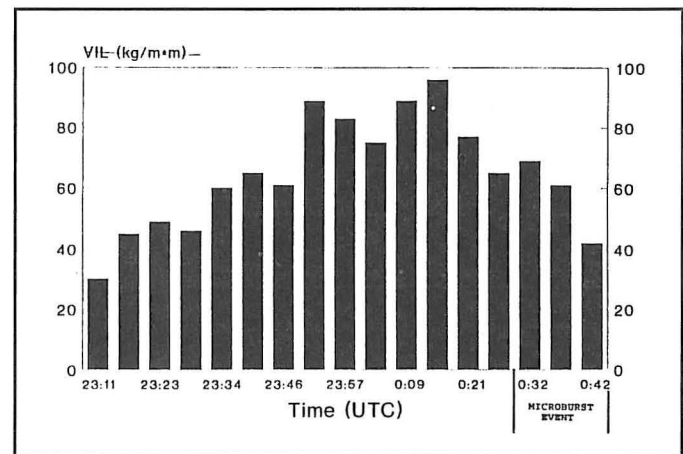

Fig. 16. Bar graph of maximum VIL (kg m^{-2}) from 2311 UTC 16 July 1993 to 0042 UTC 17 July 1993.
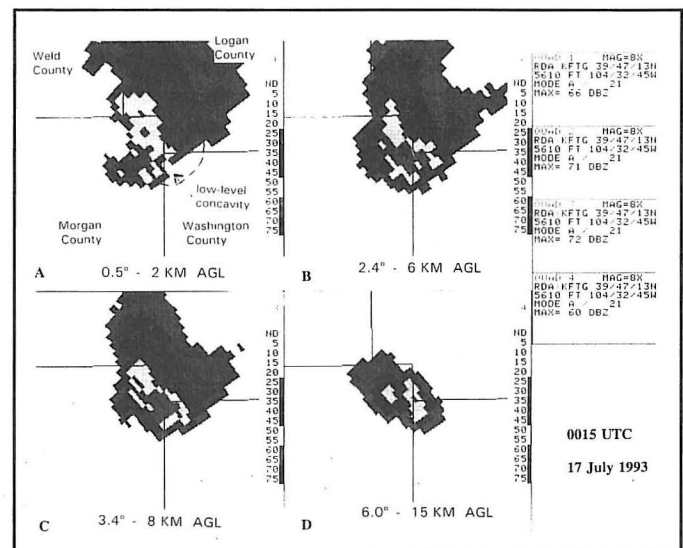

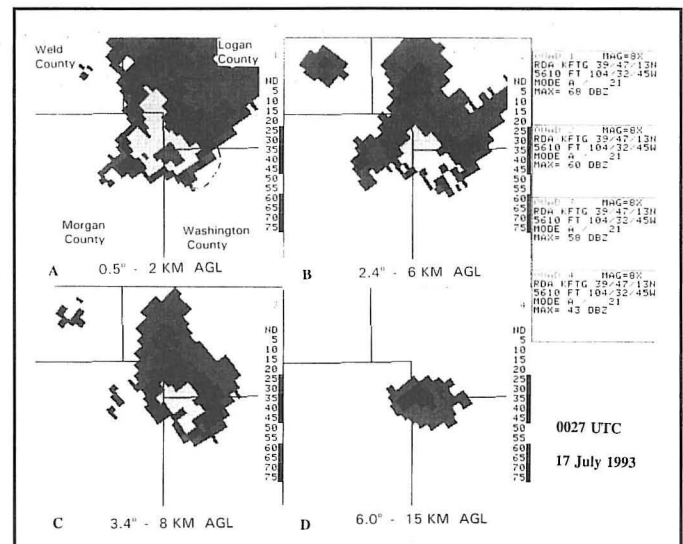Fig. 17. As in Fig. 14 except for 0015 UTC 17 July 1993. A WER is still evident.

Fig. 18. As in Fig. 14 except for 0027 UTC 17 July 1993. WER has collapsed and reflectivities at 3.4° have decreased significantly.
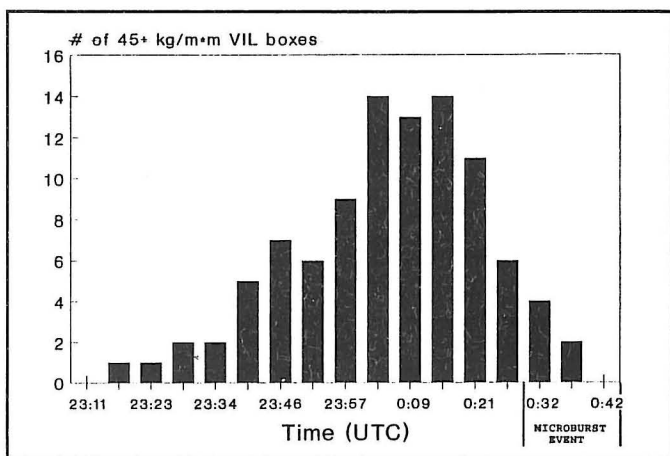
Fig. 19. Bar graph of number of VIL boxes (4 km × 4 km) >45 kg m⁻² from 2311 UTC 16 July 1993 to 0042 UTC 17 July 1993.
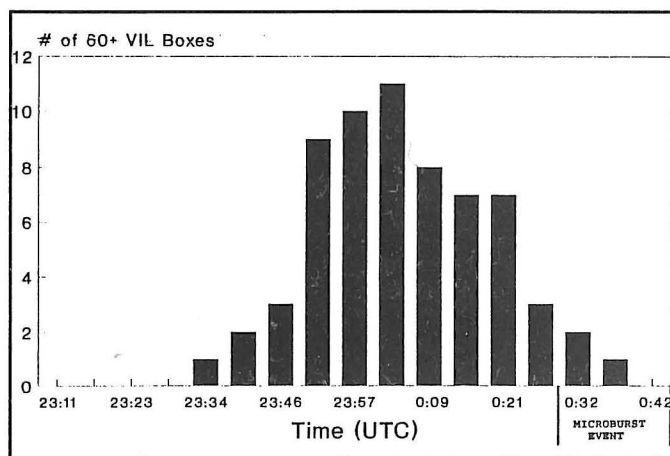

Fig. 20. As in Fig. 19 except for number of VIL boxes >60 kg m⁻².

developed. LAPS model gridded data was used to investigate the air mass farther east where there was better moisture and instability. Although the conventional surface data revealed unusually high dew points in the area, only the LAPS analyses showed a nose of high CAPE and low CIN air collocated with an area of persistent moisture convergence.

Forecasters used LAPS to generate a model-based sounding near this unstable region in real time which possessed characteristics of a wet microburst sounding. When forecasters observed an outflow boundary about to intersect a weak thunderstorm cell moving toward this unstable area, they were able to correctly anticipate rapid intensification and highlight the localized threat of severe weather through the warning process. Warnings for specific areas within the affected counties were issued 45 minutes before the deadly thunderstorm struck.

WSR-88D radar data revealed the formation of a broad and weak mesocyclone, accompanied by a WER, before the onset of the downburst. Forecasters did not anticipate tornadic activity with this storm since the storm-relative helicity and the storm's rotational shear values were weak. However, the collapsing WER and rapidly decreasing VIL values, which followed a period of increasing, extremely high VIL values with large areal coverage, led forecasters to believe that large hail and strong winds would be the main severe weather threat.

The sequence of meteorological events noted in this case can be used as an aid for determining the potential intensity of severe thunderstorms. More documented cases are needed, but if similar radar parameters are observed, the warning forecaster should word a severe thunderstorm warning more strongly than the ordinary severe thunderstorm (which typically contains only 2 cm sized hail and/or 50 kt winds). A storm with the preceding structure and evolution of VIL in a favorable microburst environment could produce wind damage that, as in this case, is as strong as an F3 (Fujita 1971) tornado.

Acknowledgments

Authors

Ron Holmes is currently the Science and Operations Officer at the National Weather Service Forecast Office in Sioux Falls, South Dakota. Prior to this position he was a journeyman forecaster at the National Weather Service Forecast Office in Denver, Colorado. His internship was completed at the Weather Service Office in Columbus, Ohio. Previous work experience includes a variety of positions in the private sector such as The Weather Channel, the Franklin Institute Science Museum in Philadelphia, and AccuWeather, Inc. He received a B.S. in Meteorology from The Pennsylvania State University in 1984. His main interests include application of research and new technology to improve operational forecasting.

Dave Imy received a B.S. in Meteorology at Texas A&M University in 1979. Dave entered the National Weather Service directly from college and has been with the organization for 16 years. He started as an intern in Little Rock, Arkansas and moved to Jackson, Mississippi in 1985 as the Warning and Preparedness Meteorologist. In 1989, he moved to Norman, Oklahoma to become an instructor for the WSR-88D Operations Training Course. Dave moved to Colorado in late 1992 as the Deputy Meteorologist-In-Charge of the Denver National Weather Service Forecast Office. His interests include all operational aspects that concern severe weather especially tornadoes.

References

Atkins, N. T., and R. M. Wakimoto, 1991: Wet microburst activity over the southeastern United States: implications for forecasting. *Wea. Forecasting,* 6, 470–482.

Benjamin, S. G., K. A. Brewster, R. Brümmer, B. F. Jewett, T. S. Schlatter, T. L. Smith and P. A. Stamus, 1991: An isentropic three-hourly data assimilation system using ACARS aircraft observations. *Mon. Wea. Rev.,* 119, 888–906.

Bleck, R., and S. G. Benjamin, 1993: Regional weather prediction with a model combining terrain-following and isentropic coordinates. Part I: Model description. *Mon. Wea. Rev.,* 121, 1770–1785.

Browning, K. A., 1965: Some inferences about the updraft within a severe local storm. *J. Atmos. Sci.,* 22, 699–677.

Burgess, D. W., and L. R. Lemon, 1990: Severe thunderstorm detection by radar. *Radar in Meteorology* (D. Atlas, Ed.) Amer. Meteor. Soc., 619–647.

Caracena, F., and M. W. Maier, 1987: Analysis of a microburst in the FACE meteorological mesonetwork in southern Florida. *Mon. Wea. Rev.,* 115, 969–985.

Colby, F. P., 1984: Convective inhibition as a predictor of convection during the AVE-SESAME II. *Mon. Wea. Rev.,* 112, 2239–2252.

Crum, T. D., and R. L. Alberty, 1993: The WSR-88D and the WSR-88D Operational Support Facility. *Bull. Amer. Meteor. Soc.,* 74, 1669–1687.

Donaldson, R. J. Jr., 1970: Vortex signature recognition by a Doppler radar. *J. Appl. Meteor.,* 9, 661–670.

Doswell, C. A. III, 1980: Synoptic scale environments associated with high plains thunderstorms. *Bull. Amer. Meteor. Soc.,* 61, 1388–1400.

——————, 1985: Temporal evolution of 700-500 mb lapse rate as a forecasting tool—a case study. Preprints, *14th Conf. Severe Local Storms,* Amer. Meteor. Soc., Indianapolis, 398–401.

——————, 1987: The distinction between large-scale and mesoscale contributions to severe convection: a case study example. *Wea. Forecasting,* 2, 3–16.

Foster, D. S., 1958: Thunderstorm gusts compared with computed downdraft speeds. *Mon. Wea. Rev.,* 86, 91–94.

Fujita, T. T., 1971: A proposed characterization of tornadoes and hurricanes by area and intensity. Satellite and Mesometeorology Research Project Report No. 91, Dept. of Geophysical Sciences, Univ. of Chicago, 5734 S. Ellis Ave., Chicago, IL 60637, 42 pp.

Green, R. G., and R. A. Clark, 1972: Vertically Integrated Liquid water—A new analysis tool. *Mon. Wea. Rev.,* 100, 548–552.

Hart, J. A. and W. D. Korotky, 1991: The SHARP workstation version 1.5. A Skew-t/Hodograph Analysis and Research Program for the IBM and compatible PC. *NOAA Eastern Region Computer Programs,* National Weather Service, Bohemia, NY, 58 pp.

Imy, D. A., and K. J. Pence, 1992: An examination of a high-precipitation supercell using a tilt sequence with the WSR-57.

Proceedings, *Tornado Symposium III* (C. Church, Ed.), Amer. Geophys. Union, 257–264.

Klazura, G. E., and D. A. Imy, 1993: A description of the initial set of analysis products available from the NEXRAD WSR-88D System. *Bull. Amer. Meteor. Soc.,* 74, 1293–1311.

Lemon, L. R., 1980: New severe thunderstorm radar identification techniques and warning criteria. NOAA Tech. Memo. NWS NSSFC-3 [NTIS Accession No. PB-273049], 60 pp.

McGinley, J. A., S. C. Albers, and P. A. Stamus, 1991: Validation of a composite convective index as defined by a real time local analysis system. *Wea. Forecasting,* 6, 337–356.

Modahl, A. C., 1979: Low level wind and moisture variations preceding and following hailstorms in northeast Colorado. *Mon. Wea. Rev.,* 107, 442–450.

Przybylinski, R. W., J. T. Snow, and J. T. Curran, 1992: The use of volumetric radar data to identify supercells: a case study of June 2, 1990. Proceedings, *Tornado Symposium III* (C. Church, Ed.), Amer. Geophys. Union, 241–250.

Srivastava, R. C., 1985: A simple model of evaporatively driven downdraft: application to microburst downdraft. *J. Atmos. Sci.,* 42, 1004–1023.

Toth, J. J., and R. H. Johnson, 1984: Summer flow characteristics over northeast Colorado. *Mon. Wea. Rev.,* 113, 1458–1469.

Wakimoto, R. M., and V. N. Bringi, 1985: Forecasting dry microburst activity over the high plains. *Mon. Wea. Rev.,* 113, 1131–1143.

——————, 1988: Dual-polarization observations of microbursts associated with intense convection: the 20 July storm during the MIST project. *Mon. Wea. Rev.,* 116, 1521–1539.

Winston, H. A., and L. J. Ruthi, 1986: Evaluation of RADAP II severe storm detection algorithms. *Bull. Amer. Meteor. Soc.,* 67, 145–150.

USDC, 1993: *Storm Data.* Vol. 35, No. 7, National Climatic Data Center, 300 pp.